



Validation of satellite-based noontime UVI with NDACC ground-based instruments: influence of topography, environment and overpass time

Colette Brogniez¹, Frédérique Auriol¹, Christine Deroo¹, Antti Arola², Jukka Kujanpää³, Béatrice Sauvage^{1*}, Niilo Kalakoski³, Mikko R.A. Pitkänen², Maxime Catalfamo¹, Jean-Marc Metzger⁴, Guy
5 Tournois⁵, Pierre Da Conceicao⁵

¹Laboratoire d'Optique Atmosphérique, Université Lille 1 Sciences et Technologies, 59655 Villeneuve d'Ascq, France

²Finnish Meteorological Institute, Yliopistonranta 1 F, P.O. Box 1627, FI-70211 Kuopio, Finland

³Finnish Meteorological Institute, Earth Observation Unit, P.O. Box 503, FI-00101 Helsinki, Finland

⁴UMS 3365 - OSU Réunion, Université de La Réunion, St-Denis de La Réunion, France

10 ⁵UMS 3470 - OSU Pytheas, Observatoire de Haute Provence, St-Michel l'Observatoire, France

* No more at LOA

Correspondence to: Colette Brogniez (colette.brogniez@univ-lille1.fr)

Abstract. Spectral solar UV radiation measurements are performed in France using three spectroradiometers located in very different sites. One is installed in Villeneuve d'Ascq, in the north of France (VDA). It is an urban site in a topographically
15 flat region. Another instrument is installed in Observatoire de Haute Provence, in the French Southern Alps (OHP). It is a rural mountainous site. The third instrument is installed in Saint-Denis, Reunion Island (SDR). It is a coastal urban site on a small mountainous Island in the Southern tropics. The three instruments are affiliated to the Network for the Detection of Atmospheric Composition Change (NDACC) and carry out routine measurements to monitor the spectral solar UV radiation and enable derivation of UV index (UVI). The ground-based UVI values observed at solar noon are compared to similar
20 quantities derived from OMI/Aura and GOME-2/Metop-A satellite measurements for validation of these satellite-based products. The present study concerns the period 2009-september 2012, date of the change of OMI data processing. UVI products from the old (v1.2) and new (v1.3) versions of OMI are used to assess the improvement of the new processing. On average, estimates from satellite instruments always overestimate surface UVI at solar noon. Under cloudless conditions the satellite-derived estimates of UVI compare satisfactorily with ground-based data: the median relative bias is less than 8 % at
25 VDA and 4 % at SDR for both OMI-v1.3 and GOME-2, and about 6 % for OMI-v1.3 and 2% for GOME-2 at OHP. Correlation between satellite-based and ground-based data is better at VDA and OHP (about 0.99) than at SDR (0.96) for both spatial instruments. For all sky conditions the median relative biases are much larger, with large dispersion for both instruments at all sites (VDA: about 12 %; OHP: 9 %; SDR: 11 %). Correlation between satellite-based and ground-based data is still better at VDA and OHP (about 0.95) than at SDR (about 0.73) for both satellite instruments. These results are
30 explained considering the time of overpass of the two satellites, which is far from solar noon, preventing a good estimation of the cloud cover necessary to a good modelling of the UVI. Site topography and environment are shown to have a non-significant influence. At VDA and OHP, OMI-v1.3 shows a significant improvement with respect to v1.2 that did not account for absorbing aerosols.



1 Introduction

35

Monitoring of UV solar radiation at the surface is a necessary and important task to characterize the impact of atmospheric composition change, as is a goal for example of the Network for the Detection of Atmospheric Composition Change (NDACC) and of the Global Atmosphere Watch Programme (GAW). Indeed UV radiation affects the biosphere having both benefits and risks (detrimental effects) whose relative importance depends strongly on latitude and season. Currently, approximately 30 sites in the northern hemisphere and only 8 in the southern hemisphere perform spectral UV measurements. Observations at northern mid-latitudes help complete geographical coverage. Observations from Reunion Island, close to the tropic of Capricorn, are useful as well.

40

Due to the scarcity of surface-based UV measurements, which results in sparse geographical coverage, satellite platforms are very useful since they provide global data. Surface UV radiation from satellite radiance measurements is retrieved via radiative transfer codes whose input data are ozone and aerosol contents, surface albedo and cloudiness. Some of these data are products of the instrument itself (ozone, cloudiness) while others come from climatologies (aerosol content, albedo). Differences between the two satellite instruments that will be used in this work (OMI and GOME-2) are detailed below.

45

Despite their extensive geographical coverage, satellite-based (SB) data products are affected by measurement uncertainties, as are ground-based (GB) products. However, SB data are also affected by modelling uncertainties. Moreover due to their rather coarse spatial resolution, SB data sometimes do not capture fine scale phenomena. Thus, GB measurements are essential for validation of finer scale satellite measurements. Overall, various sites are useful for assessing the satellite data products in various conditions, including various latitude, land cover, altitude and climate. However, validation exercises are difficult to achieve due to differences in temporal and spatial resolutions of GB and SB data products. Extensive comparison studies between surface UV provided by OMI and GB measurements have been previously made (Tanskanen et al., 2007, Buchard et al., 2008, Ialongo et al., 2008, Weihs et al., 2008). Those studies dealt with version 1.2 which did not account for the influence of absorbing aerosols, implying a positive bias in OMI product. The OMI product has been tentatively corrected by several methods (Kazadzis et al., 2009a and 2009b, Arola et al., 2009, Anton et al., 2012, Muyimbwa et al., 2015). From the comparisons against GB measurements, the OMI surface UVI at sites with low amounts of absorbing aerosols has been shown to be an overestimation of 0–10%. Alternatively, at sites with significant influence from absorbing aerosols, OMI surface UVI show a larger positive bias of up to 50%. All these OMI validations were conducted using data collected at the time of the satellite overpass. Currently only one validation study is available for GOME 2, but it only concerns daily doses (Kalakoski, 2009). For both satellite instruments these validations address data up to 2008 (except for OMI in Anton et al., 2012 and Muyimbwa et al., 2015). In the present study validations are conducted over a more recent period at three French sites, including a new southern site.

50

60

65

Saint-Denis site, Reunion Island, is characterized by a complex topography and by a frequent occurrence of orographic clouds forming at around midday. Due to its tropical location (high sun elevation in summer and low total ozone column) the UV radiation level is very high. Overpass by OMI occurs in the afternoon and GOME-2 overpass occurs in the morning. The



two other metropolitan sites are characterized by the presence of absorbing aerosols, on average in larger quantity in Villeneuve d'Ascq than in Observatoire de Haute Provence, but less absorbing. Their mid-latitude situation implies lower UV radiation levels than in the tropics (lower sun elevation in summer and larger total ozone column). For both sites, overpass occurs close to noontime for OMI and in the morning for GOME-2.

OMI and GOME-2 websites make available UVI data and maps at solar noon, when values are generally close to the maximum, therefore confrontation with ground-based UVI is carried out in this study at noontime. Validations of satellite-based estimates with ground-based measurements are conducted under cloudless and all sky conditions during about four years (January 2009-September 2012, date of the replacement of OMI version 1.2 by version 1.3). Both versions of OMI data are used to assess the effect of the absorbing aerosol correction that has been recently introduced (v1.3 available since end of March 2014). The influence of the cloudiness assumed by each satellite algorithm on the SB-GB UVI comparison is discussed. The influence of the site topography and environment is studied as well.

The ground-based spectroradiometers and the OMI and GOME-2 instruments are described in Sect. 2 along with the methodologies for deriving surface UVI. Section 3 presents the comparisons between the satellite-based and the ground-based UVI in various conditions. Conclusions are listed in Section 4.

2 Instruments

2.1 Ground-based

2.1.1 Description

The UV measurements used here come from three French stations: Villeneuve d'Ascq (50.61° N, 3.14° E, 70 m above sea level (a.s.l.), referred to as VDA in the following), Observatoire de Haute Provence (43.93° N, 5.70° E, 686 m a.s.l., referred to as OHP) and Saint-Denis, Reunion Island (20.9° S, 55.5° E, 85 m a.s.l., referred to as SDR). The three sites are each equipped with a double monochromator Bentham DTMc300. The instruments are thermally regulated. They provide global irradiance spectra in the 280-450 nm wavelength range with a 0.5 nm sampling step and a Full Width at Half Maximum (FWHM) of about 0.5 nm. Scans are performed every fifteen minutes (at SDR and OHP in 2009-2010), or thirty minutes (at VDA and OHP in 2011-2012). Scan duration is about 5 minutes.

2.1.1 Data processing

The instruments are regularly calibrated with standard 1000W lamps traceable to National Institute of Standards and Technology. After calibration, the wavelength misalignment is corrected via a software tool developed at Laboratoire d'Optique Atmosphérique (Houët, 2003) and improved during an intercomparison campaign with the QASUME (Quality Assurance of Spectral Ultraviolet Measurements in Europe) instrument held in 2010. The cosine correction is then carried out leading to the "measured" irradiance I at wavelength λ .



The erythemally weighted UV, UV_{ery} , is obtained by integrating over the wavelength the irradiance $I(\lambda)$ weighted by the erythema action spectrum $A(\lambda)$. The erythema action spectrum used is from CIE (Diffey and McKinlay, 1987). The UV index is then derived by dividing UV_{ery} (in Wm^{-2}) by $25 \cdot 10^{-3} Wm^{-2}$.

105 Irradiance uncertainty results from uncertainties in the absolute calibration (including spectral irradiance lamp uncertainty provided by the lamp supplier, imprecision of adjustments and wavelength misalignment) and in the field measurements (imprecision of diffuser horizontality, uncertainty in cosine correction and in wavelength shift correction).

The irradiance uncertainty leads to an UVI uncertainty for a coverage factor $k = 2$ of about 5 %.

All instruments are affiliated to NDACC.

110

2.2 Satellite-based

2.2.1 OMI

115 Description

The Ozone Monitoring Instrument (OMI) on Aura platform, launched on July 2004 into a sun-synchronous quasi-polar orbit, is a nadir-viewing UV/visible spectrometer dedicated to the monitoring of atmospheric ozone, trace gases, aerosol, cloudiness and surface UV. OMI measures the solar radiation backscattered by the atmosphere with a spectral resolution of about 0.45 nm in the UV and a spatial resolution at nadir of 13 km (along track) x 24 km (across track) (Levelt et al., 2006).

120 Thanks to Aura orbit and large OMI swath width of 2600 km, the daily geographic coverage is global.

Data processing

The OMI version 1.2 algorithm first estimates clear-sky surface UV irradiance via a radiative transfer model using total ozone column, derived from measurements of OMI itself via another dedicated algorithm, surface albedo provided by a climatology (Tanskanen, 2004), a high-resolution extraterrestrial solar spectrum and climatological profiles of ozone and temperature (Krotkov et al., 2002). Secondly, non-absorbing aerosols and cloud cover are accounted for as a correction factor to estimate the actual surface UV radiation. The cloud cover parameter used is the cloud optical depth (COD) determined from OMI measurements. For products estimated at local noontime, change in cloudiness between the OMI local overpass time and noontime is not taken into account. This modelling is performed for solar zenith angles (SZA) lower than 130 85°. Finally, UVI is derived from spectral irradiance.

OMI-derived UVI data used here come from the OMUVB product available for overpass sites from <http://avdc.gsfc.nasa.gov/index.php?site=595385375&id=79>.

According to earlier validation works performed with OMI version 1.2 (Arola et al., 2009, Kazadzis et al., 2009a and 2009b, Anton et al., 2012), the high positive bias between OMI-UVI and GB data is due to absorbing aerosols. The new version 1.3



135 accounts for absorbing aerosols via an aerosol climatology (Kinne et al., 2013), which is used in a correction factor (CF) applied to v1.2 UV estimates (Arola et al., 2009).

Uncertainty in OMI-derived UVI is due to uncertainties in the clear-sky irradiance modelling (depending on ozone, surface albedo) and in the cloud-aerosol correction factor. According to Krotkov et al. (2002), the resulting uncertainty is about 5 % (10 % for $k = 2$) in clear sky conditions and about 7 % (14 %) in cloudy conditions. When the satellite overpass occurs at a
140 time significantly different from local noon, an additional uncertainty is added because UVI is given at noontime and the correction factor estimated at the time of the overpass. In presence of absorbing aerosols, the estimated uncertainty for v1.2 increases to about 15-25 % (30-50 %), depending on aerosol type and load. In the latest version, this systematic overestimation has been significantly reduced. According to Arola et al. (2009), the use of the absorbing aerosol correction results in a significantly reduced bias by 5–20 %.

145

2.2.2 GOME-2

Description

150 The second Global Ozone Monitoring Experiment (GOME-2) on Metop-A platform was launched on October 2006 into a sun-synchronous quasi-polar orbit. The spectrometer is nadir-scanning measuring the solar radiation backscattered by the atmosphere with a spectral resolution of about 0.27 nm in the UV. In the default scanning mode, the swath width is 1920 km enabling global coverage in 1.5 days. The spatial resolution is 40 km (along track) x 80 km (across track). The spatial resolution is kept constant throughout the swath by adjusting the speed of the scanning mirror (Munro, 2015).

155

Data processing

The GOME-2 algorithm proceeds similarly to OMI algorithm, with slight differences. Surface UV irradiance is estimated via a radiative transfer model using total ozone column, derived from GOME-2 measurements via another dedicated algorithm,
160 surface albedo from the same climatology as the OMI algorithm, an extraterrestrial solar spectrum, climatological profiles of ozone, temperature, aerosols and clouds (Kujanpää and Kalakoski, 2015). Aerosol properties come from Global Aerosol Data Set (GADS) data (Koepke et al., 1997) and aerosol optical thickness comes from the climatology of Kinne (2007). Instantaneous cloud optical thickness (COD) is derived via interpolation of COD retrieved from measurements of AVHRR-3/Metop-A (which is on the same platform as GOME-2, having a morning orbit and the same local overpass time) and
165 AVHRR-3 aboard NOAA satellites on the afternoon orbit (NOAA-18 until 3 June 2009, and then on NOAA-19). Depending on the station latitude, two or more AVHRR overpasses occur making two or more COD values available. All input data are mapped to a regular $0.5^\circ \times 0.5^\circ$ latitude-longitude grid. UVI is derived from spectral irradiance and given in the same grid. For the current study, O3M SAF offline surface UV (OUV) products were reprocessed using the algorithm version 1.13 with a special option to store diurnal COD values, which are not included in the standard product.



170 Uncertainty in GOME-2-derived UVI is due to uncertainty in the irradiance modelling (depending on ozone, surface albedo,
cloud and aerosols). The resulting uncertainty is about 8 % (16 %) in clear sky conditions and about 10-20 % (20-40 %) in
cloudy conditions, depending on the number of COD values available. As for OMI, the largest contribution to the
uncertainty comes from the cloudiness estimate because UVI is given at noon rather than at the satellite overpass time. In
presence of absorbing aerosols, the uncertainty increases to about 30-35 % (60-70 %), depending on aerosol type and content
175 (Kujanpää, 2013).

3 Results

Due to their limited spatial resolution, space-borne measurements represent an average value for the observed pixel. Thus,
180 when cloud cover is not homogenous in the pixel, satellite data should not be directly compared to instantaneous ground-
based measurements. For comparison at overpass time, the effect of the cloud variability within a satellite sensor pixel can
be accounted for by averaging GB measurements over a time interval around the time of overpass. Here, comparisons are
conducted at noontime, and the cloudiness used in OMI and GOME-2 algorithms are not actual values at noontime.
Nevertheless, in all sky conditions (AS), GB UVI have been averaged over a time interval around noontime. Several time
185 intervals have been tested and hourly average of GB values has been selected as being better representative of spatial
measurements for both space-borne instruments. Though GOME-2 pixel is larger than OMI pixel a mean over a larger time
interval is not valuable since it would introduce a low bias in the GB product at solar noon (indeed, UVI is generally
maximum at noon).

In cloudless conditions (CS), to avoid introducing a low bias in the GB product at solar noon (see above), no average has
190 been made. The selection of CS measurements at noontime cannot be made via cloud information available in the OMI data
files since the COD corresponds to overpass time, for GOME-2 cloud information is interpolated at noon from AVHRR data
(see section 2.2.2), therefore the COD value maybe not really valid. Thus, CS selection is based on the examination of the
GB-UVI measurements. Two criteria are set up to declare the sky as “cloudless”: (i) the shape of the curve of the UVI
diurnal variations around noon must be smooth, and (ii) the UVI relative dispersion around the hourly mean must be less
195 than 5 %, this value being an estimate of the UVI variation due to SZA variation around noontime (estimation derived from
modelling). In addition, SEVIRI/MSG images must show cloud free conditions close to the measurement time. This method
is not perfect because a nearly constant cloud cover can be mistaken for cloud free.

One has considered two limits for the distance between the GB station and the cross track position (CTP) for OMI and the
grid cell centre point for GOME-2.

200 Satellite-based and ground-based datasets are compared by computing the UVI difference (SB-GB), the UVI relative
difference (SB-GB)/GB expressed in per cent, and by plotting correlation diagrams of UVI. The following statistics
parameters were used to quantify the agreement: mean and median difference, mean and median relative difference, root-
mean square difference, root-mean square relative difference, standard deviation, as described in Appendix, correlation



coefficient and equation of the regression line obtained via a bivariate least squares method (York et al., 2004). These
205 statistical parameters are common in such validation studies (for example: Tanskanen et al. (2007), Ialongo et al. (2008),
Weihs et al. (2008), Kalakosky (2009), Kazadzis et al. (2009a), Muyimbwa et al. (2015)).

The comparisons between SB and GB UVI are first carried out considering all the UVI pairs for each satellite sensor and
various conditions (100 km and 10 km for the limit distance, filter on altitude). Then, to enable a comparison of the
performances of the satellite sensors an additional study restricted to common dates is conducted.

210

3.1 VDA

At this northern mid-latitude site, OMI overpasses occur from 0.5 h before to 2.5 h after solar noon. The GOME-2
overpasses take place in the morning from 3 h to 0.5 h before solar noon. VDA site, located in a topographically flat region,
215 is characterized by rather high total ozone columns (on average in the 250-450 DU range) and by the presence of absorbing
aerosols of pollutant origin. The surface albedo at 360nm, provided in the OMUVB database, exhibits a weak seasonality in
the [0.03-0.07] range.

For both satellite instruments, the distance between the ground station and the CTP/grid cell centre point is first chosen
smaller than or equal to 100km.

220 Comparison results for AS conditions are shown in Fig. 1 for both satellite instruments, the upper panels present OMI-v1.3,
and the lower panels GOME-2. Histograms of the per cent relative differences between SB and GB UVI data are located to
the left and correlation diagrams are located to the right. Crosses circled with blue (for OMI) or turquoise (GOME-2)
correspond to COD less than or equal to 1. Notice that the GOME-2 data set is smaller than the OMI data set because there is
only one value per day and no value when SZA at noon is larger than 70°. The data show a medium dispersion around
225 relative difference means (STD nearly 40., means nearly 21.), the correlation between SB and GB UVI is strong (correlation
coefficients $r \sim 0.95$) and the regression lines have a slope larger than unity (1.08 ± 0.01 for OMI, 1.12 ± 0.01 for GOME-
2) with a small intercept. Satellite-derived UVI is larger than GB-derived UVI (positive relative difference) in 78 % of cases
for OMI and in 73 % for GOME-2. When the COD is smaller than or equal to 1 (circled crosses) the UVI relative difference
is almost always positive for OMI (Fig 1b), but is less so for GOME-2 (Fig. 1d). Satellite-derived UVI smaller than GB-
230 derived UVI (negative relative difference) can occur when the COD is large, as seen in Fig. 3a and 3c where the UVI relative
difference is plotted versus the COD retrieved from satellite instruments. These negative UVI relative differences for large
COD are observed for both low and high UVI ($UVI \geq 3$: for OMI blue circles, for GOME-2 green circles), especially for
OMI. Negative UVI differences for small COD ($COD \leq 1$) are sometimes observed for GOME-2, which can be related to the
SZA at the time of satellite overpass. Indeed, as seen in Fig. 4a and 4c, a filter set up on SZA at overpass shows that when
235 $SZA > 60^\circ$ correspond to $UVI < 3$ and to many negative relative differences for both OMI and GOME-2 (blue and green
circles). Approximate values of the median relative biases are 12.5 % for OMI and 12.1 % for GOME-2.



Figure 2 shows the results obtained in CS conditions. The dispersion around relative difference means is weak (STD<10., means<8.), the correlations between SB and GB UVI are very strong ($r\sim 1$), and the slopes of the regression lines are slightly larger than in AS conditions (1.10 ± 0.01 for OMI, 1.14 ± 0.02 for GOME-2) with small intercepts. Satellite-derived UVI is still generally larger than GB-derived UVI (~ 92 % of cases for OMI, 80 % for GOME-2) and this corresponds almost always to COD ≤ 1 (circled crosses), as seen also in Fig. 3b and 3d. These low COD indicate the satellite algorithms provide a good estimate of the actual cloudiness. As for GOME-2 in AS conditions, for UVI values smaller than about 3 GOME-2 values are generally smaller than GB values (Fig. 3d), and these cases correspond to SZA $> 60^\circ$ (Fig. 4d). Only two such cases are observed for OMI (Fig. 3b and 4b). Both satellite sensors demonstrate a positive median relative bias (SB-UVI $>$ GB-UVI) of 8.4 % for OMI and 8.3 % for GOME-2. Even though the number of CS cases is not large for GOME-2 comparison (37), the results are reliable.

The statistics results are reported in Table 1 for AS conditions and in Table 2 for CS conditions. The median bias is positive for both instruments and small: 0.21 for OMI and 0.33 for GOME-2 in AS conditions, 0.32 for OMI and 0.39 for GOME-2 in CS conditions.

A seasonal effect is observed on differences for both instruments with smaller values in winter, which correspond to weak UVI. UVI relative differences for OMI show no seasonal effect (the large UVI differences being divided by high UVI). However, for GOME-2, UVI relative differences exhibit seasonal variations since negative values related to weak UVI and large SZA occur mostly in winter rather than in other seasons (not shown). Surface albedo seasonality seems too weak to explain this behaviour.

These performances of the two satellite instruments should not be compared because the temporal coverage is not the same. Another study enabling to conduct a comparison of the performances is carried out further.

The overpass of both satellite instruments occurs sometimes quite far from noon. Surprisingly, no correlation between the UVI relative difference and the time difference between overpass and noon is observed, neither in AS nor in CS conditions (not shown).

The impact of the distance between the ground station and the CTP/grid cell centre point appears to be negligible. Tables 3 and 4 report results for distances smaller than or equal to 10 km. For both OMI and GOME-2, the number of UVI pairs (SB-GB) is much smaller than when considering 100 km distance. For AS conditions, the correlation between SB UVI and GB UVI data is hardly stronger for both satellite instruments (correlation coefficient increased by 0.01). Regression line slopes are closer to 1 than for 100 km case (1.06 ± 0.02 for OMI, 1.10 ± 0.03 for GOME-2). However, relatively large uncertainties limit significance of these differences. The values of the statistics parameters indicate an agreement close to that obtained for 100 km (median UVI relative bias for OMI of 10.3 % instead of 12.5 %, median relative bias for GOME-2 of 14.3 % instead of 12.1 %). For CS conditions correlation between OMI UVI and GB UVI is the same as for 100 km, the slope is almost unchanged (1.09 ± 0.01), the statistics parameters indicate better agreement (median relative bias 6.6 % instead of 8.4 %), though these results are less reliable than for 100 km because there are only 14 UVI pairs. No study can be



270 conducted for GOME-2 (only 2 pairs). Thus, a satellite validation performed with shorter distances between the satellite CTP/grid cell centre point and the GB instrument does not change significantly the results.

Finally, for AS conditions about 56 % of OMI and GOME-2 UVI data agree with GB data in the interval [-20 %; 20 %] (30 % agree in [-10 %; 10 %]). For CS conditions 100 % of OMI UVI data and 95 % of GOME-2 UVI data agree with GB data in the interval [-20 %; 20 %] (60 % agree in [-10 %; 10 %]).

275 As mentioned above, an additional study compares the performances of the two instruments on common dates. Tables 5 and 6 report the results. In AS conditions, the correlation between SB and GB UVI is strong ($r \sim 0.95$) for both satellite instruments, the slopes of the regression lines are significantly closer to 1 for OMI (1.05 ± 0.01) than for GOME-2 (1.12 ± 0.02), with a negative intercept for GOME-2. In CS conditions SB and GB UVI are very strongly correlated ($r \sim 0.99$) for both satellite instruments, the slopes of the regression lines are larger than in AS conditions with a smaller difference between OMI (1.10 ± 0.01) and GOME-2 (1.14 ± 0.02). The median biases and median relative biases are very close for both instruments for both AS and CS conditions.

The seasonal variability of differences between SB and GB UVI is greater for GOME-2 with frequently larger values than for OMI outside the winter period. UVI relative differences show no seasonal variability for OMI, but they do for GOME-2 because, as mentioned in the previous study, (i) the UVI differences for GOME-2 are larger than for OMI outside the winter season leading to larger relative differences for GOME-2 than for OMI and (ii) there are more negative relative difference for GOME-2 than for OMI, mainly in winter.

285 Tables 1 and 2 also report the results of the comparison of OMI-v1.2 data with GB data. Median UVI relative biases are about 21 % in AS conditions and about 18 % in CS conditions. Median UVI biases are about 0.4 in AS conditions and about 0.8 in CS conditions. In addition the slopes of the regression lines are (1.17 ± 0.01) in AS conditions and (1.20 ± 0.01) in CS conditions. Apart from the strong correlation between SB and GB UVI (nearly the same as for v1.3), all these statistics parameters are significantly different from those produced by v1.3. As expected, v1.3 product is more reliable than v1.2 one. Indeed, as observed in Fig. 5 (red plots), the aerosol optical depth (AOD) is quite large (Fig. 5a) and the single scattering albedo (SSA) is significantly smaller than unity (Fig. 5b), leading to a correction factor (CF) applied to v1.2 data to account for absorbing aerosols (see section 2.2.1) much smaller than unity (Fig. 5c). As mentioned previously, UVI relative differences in v1.3 do not exhibit seasonal variability, whereas a weak seasonal variability is observed in v1.2 (not shown), possibly related to CF seasonality. The current validation study at VDA demonstrates that v1.3 off-line correction for absorbing aerosol is very efficient, even if there remains a positive bias.

3.2 OHP

300

At this northern mid-latitude site, OMI overpasses occur from 0.25 h before to 2.75 h after solar noon and GOME-2 overpasses take place in the morning (ranging from 3.25 h to 1 h before solar noon). The OHP site, located in a mountainous



region, is characterized by rather high total ozone columns (on average in the 250-420 DU range) and sometimes by the presence of absorbing aerosols. Surface albedo has a weak seasonal variability in the [0.02-0.05] range.

305 The first validation is conducted for distance between the GB station and the CTP/grid cell centre point ≤ 100 km. Results for AS conditions are shown in Fig. 6. Similar to VDA, GOME-2 data set is limited because only one value per day is available. The data show medium dispersion around relative difference means (STD nearly 50., means nearly 21.), GB and SB UVI are strongly correlated ($r \sim 0.96$) and regression lines have a slope larger than unity (1.04 ± 0.01 for OMI, 1.05 ± 0.01 for GOME-2) with a small intercept. Similar to VDA, satellite-derived UVI is generally larger than GB-derived UVI (82 % of positive relative difference for OMI, 72 % for GOME-2). When the COD is smaller than 1 the relative difference is almost always positive for OMI (Fig 6b), but is less so for GOME-2 (Fig. 6d). Negative differences for large

310 UVI (82 % of positive relative difference for OMI, 72 % for GOME-2). When the COD is smaller than 1 the relative difference is almost always positive for OMI (Fig 6b), but is less so for GOME-2 (Fig. 6d). Negative differences for large COD are observed both for low and high UVI, especially for OMI data. Again, negative differences for small COD generally correspond to low UVI (Fig. 8a and 8c) and large SZA, especially for GOME-2 (Fig. 9a and 9c). Median values of the relative biases are about 9.3 % for OMI and 8.4 % for GOME-2.

315 Figure 7 shows the results obtained in CS conditions. The dispersion around relative difference means is small (STD < 10 ., means < 6 .), SB and GB UVI are strongly correlated ($r = 0.99$), and the slopes of the regression lines are still larger than unity (1.05 ± 0.01 for OMI, 1.09 ± 0.01 for GOME-2). Note that the point well below the regression line in Fig 7b (red circled) corresponds to an OMI-CTP at 98 km distance from the GB site, 1700 m a.s.l. and to a large COD (7.75). Satellite-derived UVI is still often larger than GB-derived UVI (~ 85 % of cases for OMI, 68 % for GOME-2). The COD is generally

320 small (Fig. 8b and 8d), indicating satellite algorithms perform a good estimate of the actual cloudiness. As was the case for all sky conditions, GOME-2 UVI are generally smaller than GB UVI for UVI values smaller than about 3 (green circles), these cases correspond to SZA $> 60^\circ$ (Fig. 9d). Few such cases are observed for OMI, they correspond to a UVI close to 1 (Fig. 9b). The positive median relative bias is 5.8 % for OMI and 4.1 % for GOME-2.

The statistics results are reported in Tables 1 and 2. The median bias is positive and small for both satellite instruments: 0.32

325 for OMI and 0.41 for GOME-2 in AS conditions and about 0.25 for both OMI and GOME-2 in CS conditions.

As for VDA, seasonal variability is observed on differences for both satellite instruments with smaller values in winter. OMI relative differences show no seasonal variability, but GOME-2 relative differences exhibit seasonal variations not explained by the observed weak surface albedo seasonality.

Both satellite overpass times can be quite different from noon, however, no correlation between the relative difference and

330 the time difference is observed (not shown).

The results for distances between the ground station and the CTP/grid cell centre point ≤ 10 km are reported in Tables 3 and 4. The number of events is much smaller than in the previous study. In AS conditions, the slope of the regression line for OMI data is nearly unchanged compared to 100 km distance case (1.05 ± 0.02), the correlation coefficient and the statistics parameters (median bias and median relative bias) as well. For GOME-2 though the slope of the regression line is closer to 1

335 compared to 100 km distance and the correlation coefficient nearly unchanged, the statistics parameters are slightly worse. In CS conditions, for both OMI and GOME-2, the regression slopes are not significantly different from those for 100 km



distance, and the statistics results are very similar. Thus, the distance between the satellite CTP/grid cell centre point and the GB instrument does not affect significantly the results of the satellite sensor validation.

340 Since the region is mountainous, the effect of altitude may be evident in the data. The influence of altitude can only be studied with OMI data for which the terrain height is available in the OMUVB files. Tables 3 and 4 report the results accounting for CTP whose altitude is within +/- 250 m from the ground site altitude, this value being chosen as leading only to a +/- 2-3 % shift in erythemally weighted UV (McKenzie et al., 2001). Whether in AS or in CS conditions the statistics parameters are very close to those obtained without a filter on altitude, as well as the regression line slope and correlation coefficient. So, the altitude selection does not improve the comparisons between SB and GB data. This is likely due to OMI
345 estimated cloudiness, to OMI spatial resolution and also to the fact that CTP with lower and higher altitude than the site one give opposite effects on UVI. Indeed all these factors play a role in the validations carried out with or without an altitude selection.

Finally, for AS conditions about 70 % of OMI UVI data and about 67 % of GOME-2 data agree with GB data in the interval [-20 %; 20 %] (44 % agree in [-10 %; 10 %]). For CS conditions about 97 % of both OMI and GOME-2 UVI data agree with
350 GB data in the interval [-20 %; 20 %] (72 % agree in [-10 %; 10 %]).

The statistical comparisons restricted to the same dates for both OMI and GOME-2 are reported in Table 5 and 6. In AS conditions, the correlation between SB and GB UVI data is strong ($r \sim 0.96$) for both satellite instruments, the slopes of the regression lines are larger than 1, with no significant difference. In CS conditions the correlation is very strong ($r \sim 0.99$), the regression slope for OMI is slightly closer to 1 than for GOME-2. In AS conditions, median relative biases between GB and
355 SB UVI data are very close for OMI and GOME-2, but median absolute bias for GOME-2 is larger than for OMI. In CS conditions, the median relative bias for GOME-2 is weaker than for OMI but median absolute bias for GOME-2 is larger than for OMI. This different behaviour between median relative bias and median bias for OMI and for GOME-2 is due to the seasonality of the relative differences and differences for GOME-2 - GB UVI pairs. Indeed, the seasonal variability of differences between SB and GB UVI is greater for GOME-2 than for OMI, and, as observed for VDA, OMI relative
360 differences between SB and GB UVI show no seasonal variability, but GOME-2 relative differences do.

The statistics results of the comparison for OMI-v1.2 are also reported in Tables 1 and 2. Median relative biases are about 20 % in AS conditions and about 17 % in CS conditions. Median biases are about 0.8 in AS conditions and about 0.9 in CS conditions. The slopes of the regression lines are (1.14 ± 0.01) in AS conditions and (1.18 ± 0.01) in CS conditions. Thus, all these statistics parameters are significantly larger than those produced by v1.3, indicating that v1.3 product is more
365 reliable than v1.2 one. This result can be understood by looking in Fig. 5 (black plots). AOD is quite large (Fig. 5a) and SSA significantly smaller than unity (Fig. 5b), leading to a CF applied to v1.2 UVI much lower than unity (Fig. 5c). The current validation study at OHP shows that the correction for absorbing aerosol performed in v1.3 is very efficient, though imperfect.

370 **3.3 SDR**

In the tropical region OMI overpasses occur in the afternoon from 0.75 h to 3.5 h after solar noon and GOME-2 in the morning from 4.25 h to 2.25 h before solar noon, on average much far from noon than OMI. As mentioned previously, SDR site is characterized by rather low total ozone column (on average in the 240-300 DU range), by a complex topography and
375 by a frequent occurrence of clouds forming at around midday. Cloud variability between overpass time and noon is thus high and cloudiness estimation is the most important factor of uncertainty in deriving UVI from space measurements. As at the other sites, surface albedo has a weak seasonality in the [0.04-0.08] range.

The first validation is conducted for distance between the GB station and the CTP/grid cell centre point ≤ 100 km.

Results for AS conditions are shown in Fig. 10. Similar to other sites, GOME-2 data set is limited because only one value
380 per day is available. The data show large dispersion around relative difference means (STD nearly 57., mean nearly 29. for OMI and STD nearly 67., mean nearly 35. for GOME-2.). These dispersions and means are larger than at the two other sites. GB and SB UVI are correlated less strongly than at other sites ($r \sim 0.74$ for OMI, $r \sim 0.71$ for GOME-2), though the correlation is significant since the probability of getting by chance these r -values is lower than 0.05%. The slopes of the regression lines are much smaller than unity (0.91 ± 0.02 for OMI, 0.78 ± 0.03 for GOME-2). Satellite-derived UVI is
385 generally larger than GB-derived UVI (~ 80 % of positive relative difference for both OMI and GOME-2). When the COD is smaller than 1 the relative difference is almost always positive for both instruments (Fig. 10b and 10d). Satellite-derived UVI smaller than GB-derived UVI can occur when the COD is large, as seen in Fig. 12a and 12c. No link with SZA at overpass is observed, indeed for OMI observations SZA is almost always smaller than 60° , and for GOME-2 several cases with SZA at overpass $> 60^\circ$ occur but the relative differences are not more negative than for other cases (not shown).

390 Median values of the relative biases are about 10 % for both OMI and GOME-2.

Figure 11 shows the results obtained in CS conditions. The dispersion around relative difference means is much lower than in AS conditions (STD $< 9.$, means $< 4.$), the correlations between SB and GB UVI are high, though weaker than at the two other sites ($r = 0.96$) and the slopes of the regression lines are close to unity (1.03 ± 0.02 for OMI, 0.98 ± 0.02 for GOME-2). Several SB-GB UVI pairs show negative relative difference, which correspond to COD > 1 . As seen in Fig. 12b
395 and 12d, the COD can still be large, indicating the difficulty for both satellite algorithms to estimate the actual cloudiness (i.e. here no cloud), though the possibility of a bad selection of CS cases at the GB site cannot be excluded. One has checked that the few points far from the regression line in Fig. 11b and 11d correspond to a large COD at overpass (for OMI) or at noon (for GOME-2). Satellite-derived UVI is larger than GB-derived UVI in nearly 70 % of cases for both instruments. The positive relative bias is nearly 4% for both OMI and GOME-2.

400 All the statistics results are reported in Table 1 and in Table 2. The median bias is positive: about 0.8 in AS conditions and 0.4 in CS conditions for OMI, about 0.9 in AS conditions and 0.3 in CS conditions for GOME-2. These values are larger than at the two other sites in AS conditions because of the higher UVI levels.



A seasonal variability of the relative difference between GB and SB UVI is observed for both AS and CS conditions for GOME-2, but it seems to be related to the seasonality of the cloudiness rather than to the surface albedo seasonality (not shown).

As at the two other sites, though both satellite instruments overpass at times very far from noon, no correlation between the relative difference and the time difference is observed in AS and CS conditions (not shown).

The study performed for distances (GB station - CTP/grid cell centre point) smaller than or equal to 10 km gives results similar to that at the two other sites (Tables 3 and 4). For OMI data, in AS conditions, the statistics parameters show better agreement with GB data compared to 100 km distance case, though correlation between SB and GB UVI and regression line are nearly the same). In CS conditions, OMI data compare also slightly better with GB data than for 100 km case. For GOME-2 data, in AS conditions, statistics parameters show worse agreement between SB and GB UVI, correlation is weaker ($r \sim 0.60$) and the slope of the regression line is much smaller (0.62 ± 0.09). In CS conditions, the statistics parameters are weakly changed compared to 100 km distance, the GB and SB UVI data show the same strong correlation and the regression line slope (0.90 ± 0.07) is much smaller than for 100 km distance but the large uncertainty limits the significance of the difference. This later case is weakly reliable because only 16 UVI pairs are available. Thus, the comparison of surface UVI from OMI is improved when smaller distance between the satellite CTP and the GB instrument is considered. For GOME-2 the comparison is worse.

Reunion Island is very mountainous so the effect of surface altitude may be evident in OMI comparison. Tables 3 and 4 show the results accounting for CTP whose altitude is within the sea level and +250 m above the site altitude. Whether in AS or in CS conditions the statistics parameters are slightly worse, but not significantly, and correlation between SB and GB UVI data is similar. As for OHP site, an altitude selection does not lead to significant changes that is also likely due to the cloudiness estimate and to OMI spatial resolution.

Finally, for AS conditions about 62 % of both OMI and GOME-2 UVI data agree with GB data in the [-20 %; 20 %] relative difference interval (40 % agree in [-10 %; 10 %]). For CS conditions about 97 % of both OMI and GOME-2 data agree with GB data in the interval [-20 %; 20 %] (70 % and 80 % for OMI and GOME-2 respectively in [-10 %; 10 %]).

The statistical comparisons restricted to the same dates for both OMI and GOME-2 are reported in Tables 5 and 6. In AS conditions, the correlation between GB and SB UVI data is not very strong but it is better for OMI ($r \sim 0.74$ and $r \sim 0.70$ for OMI and GOME-2 respectively). The slopes of the regression lines are much smaller than 1, OMI slope being significantly closer to 1 (0.91 ± 0.03 for OMI, 0.78 ± 0.03 for GOME-2) and intercepts are both large and positive (larger for GOME-2). Median relative bias and absolute bias between GB and SB data are slightly smaller for OMI than for GOME-2. In CS conditions the correlations are strong and the same for both instruments ($r \sim 0.96$), both regression line slopes are close to 1 (OMI-slope >1 , GOME-2-slope <1 with a positive intercept), but accounting for the uncertainties the difference is not significant. Median relative biases and absolute bias are slightly larger for OMI than for GOME-2.



435 As mentioned previously, GOME-2 relative differences between GB and SB UVI data show a seasonal variability related to cloud presence, while there is no variability for OMI.

The validation of previous OMI v1.2 UVI data with GB data does not show significant differences, as observed in Table 1 and 2. Indeed, in AS conditions the correlation between GB and SB UVI data is slightly weaker and the regression line slope is slightly worse than for v1.3 data, but the other statistics parameters are very similar for both versions. In CS conditions, 440 the correlation between GB and SB UVI data is slightly weaker and the regression line slope is nearly the same as for v1.3 data, but the other statistics parameters are worse. Overall, these changes are weak and not significant. This could be understood because, as can be seen in Fig. 5 (blue plots). The aerosol content is small (small AOD (Fig. 5a)) and the aerosols are weakly absorbing (large SSA (Fig. 5b)). Thus the correction factor is close to unity (Fig. 5c), leading v1.3 products to be little improved compared to v1.2 at SDR.

445

4 Conclusion

Validation of satellite noon-UVI products from OMI (v1.3) and GOME-2 (v1.13) with ground-based measurements of UVI at noon has been carried out at three sites. The three sites are very different regarding the topography and the environment. 450 One is an urban site in a topographically flat region in the north of France (VDA). The second site is a rural mountainous site in the French Southern Alps (OHP). The third one is a coastal urban site on a small mountainous island in the southern tropics (SDR). Moreover the overpass of the two satellites occurs often far from solar noon at all sites, rendering the estimate of noon-UVI a challenge due to the difficulty to estimate the actual cloudiness at noontime. The sites are each equipped with spectroradiometers affiliated to NDACC.

455 Due to the mountainous topography of Reunion Island, and thus to the frequent formation of clouds, SDR site is difficult for spatial UV estimates. The two other sites encounter less diurnal cloud cover variation and thus are more favourable for UV estimates. Nevertheless, these two latter sites are hindered by aerosols of pollutant origin whose absorption should be accounted for in the satellite algorithms.

OMI-v1.3 UVI products, derived from v1.2 products using a correction factor to account for absorbing aerosols, show much 460 better agreement with GB UVI measurements at VDA and OHP. The relative bias between SB and GB data is reduced by about 10 %, in agreement with Arola et al. (2009). OMI-v1.3 off-line correction uses a climatology for aerosol optical properties, so a reduction of the remaining positive OMI bias might be obtained via a better characterisation of these aerosol properties, for example from simultaneous measurements. This recommendation is worth also for GOME-2.

465 For the three sites, the distance between the GB site and the CTP/grid cell centre point as well as the environment topography are not critical, likely because of the rather coarse spatial resolution of the satellite instruments.

Considering the statistics parameters when the comparison of SB and GB UVI data is restricted to common dates, one observes that, in AS conditions, absolute bias and regression line slope are slightly worse for GOME-2 than for OMI at all



sites, while relative bias and correlation coefficient are similar for both satellite instruments. In CS conditions, the three sites give different results. Indeed, in terms of absolute bias OMI and GOME-2 UVI products compare with GB data equally at
470 VDA and OHP, while at SDR site GOME-2 UVI agree with GB data better than OMI UVI. In terms of median relative bias OMI and GOME-2 data agree with GB data equally at VDA, while it is slightly better at OHP and SDR for GOME-2. This later behaviour means that the absence of clouds at noon (CS conditions) is slightly better forecast by GOME-2 via COD estimates in the morning and in the afternoon. Though, the differences are subtle and globally the algorithms work equally well.

475 On average the median relative biases are in the [8.4 % - 12.5 %] and [3.8 % - 8.4 %] ranges for AS and CS conditions respectively. Thus, accounting for the uncertainties in their UVI data (see Sect. 2), satellite-based and ground-based measurements agree in AS conditions and the agreement is good in CS conditions. One could even suggest that OMI and GOME-2 uncertainties (see sections 2.2.1 and 2.2.2 respectively) are overestimated.

480 Finally the UVI estimates derived from satellite sensors OMI and GOME-2 are only weakly biased high (on average less than 0.5 unit of UVI at VDA and OHP and less than 1. at SDR), and thus are quite reliable.

Team list

Antti.Arola@fmi.fi; Frederique.Auriol@univ-lille1.fr; colette.brogniez@univ-lille1.fr; maxime.catalfamo@univ-lille1.fr;
485 pierre.daconceicao@osupytheas.fr; christine.deroo@univ-lille1.fr; Niilo.Kalamoski@fmi.fi; Jukka.Kujanpaa@fmi.fi; jean-marc.metzger@univ-reunion.fr; mikko.pitkanen@fmi.fi; work.beatrice.sauvage@gmail.com; guy.tournois@osupytheas.fr;

Copyright statement

Code availability

490

Data availability: Spectroradiometer measurements are currently available at <http://www-loa.univ-lille1.fr/index.php/observation/sites.html> and will be available soon at <ftp://ftp.cpc.ncep.noaa.gov/ndacc/station/>
OMI data are available at <http://avdc.gsfc.nasa.gov/index.php?site=595385375&id=79>. GOME-2 data are available at http://o3msaf.fmi.fi/offline_access.html.

495

500



Appendix: Statistics definitions for n pairs of UVI data

Difference: $diff_i = SB_i - GB_i$

505 Mean Bias (mean difference): $mBias = \frac{1}{n} \sum_{i=1}^n diff_i$

Root-Mean-Square difference: $RMS = \sqrt{\frac{1}{n-1} \sum_{i=1}^n (diff_i)^2}$

Relative difference in %: $rdiff_i = 100 \times \frac{SB-GB_i}{GB_i}$

Mean Relative Bias (mean relative difference) in %: $mrBias = \frac{1}{n} \sum_{i=1}^n rdiff_i$

Root-Mean-Square relative difference: $rRMS = \sqrt{\frac{1}{n-1} \sum_{i=1}^n (rdiff_i)^2}$

510 A RMS (rRMs) close to mBias (mrBias) means that the differences (relative differences) are mostly positive

Standard deviation of the relative differences (dispersion around the mean): $STD = \sqrt{\frac{1}{n-1} \sum_{i=1}^n (rdiff_i - Mean)^2}$

Median: mid-value of the differences (in UVI) or of the relative differences (in %). Median values are useful when data distributions are skewed

515

Author Contributions

C.B. and F.A. oversaw the measurements. C.B. prepared the manuscript with contributions from A.A., J.K., F.A., M.R.A.P.
 520 and N.K.. The instruments were operated by F.A., M.C., J.M.M., G.T. and P.D.C.. C.D. contributed to collecting data and processing them. C. B., A. A., J. K., M.R.A.P., N. K. and B. S. contributed to the analysis of the results.

Acknowledgements

C.B. thanks L. Labonnote (LOA) for helpful discussions and R. De Filippi for automation of data transfer. The sites are
 525 supported by CNES within the French program TOSCA. SDR site is also supported by “la région La Réunion”. Development of the OUV product has been partly funded by EUMETSAT.



References

- Antón, M., Piedehierro, A.A., Alados-Arboledas, L., Wolfran, E., and Olmo, F.J.: Extreme ultraviolet index due to broken
530 clouds at a midlatitude site, Granada (southeastern Spain), *Atmospheric Environment*, vol. 118, p. 10-14, 2012.
- Arola, A., Kazadzis, S., Lindfors, A., Krotkov, N., Kujanpää, J., Tamminen, J., Bais, A., di Sarra, A., Villaplana, J. M.,
Brogniez, C., Siani, A. M., Janouch, M., Weihs, P., Webb, A., Koskela, T., Kouremeti, N., Meloni, D., Buchard, V.,
Auriol, F., Ialongo, I., Staneck, M., Simic, S., Smedle, A., and Kinne, S.: A new approach to correct for absorbing
aerosols in OMI UV, *J. Geophys. Res.*, vol. 36, L22805, doi: 10.1029/2009GL041137, 2009.
- 535 Buchard, V., Brogniez, C., Auriol, F., Bonnel, B., Lenoble, J., Tanskanen, A., Bojkov B., and Veeffkind, P.: Comparison of
OMI ozone and UV irradiance data with ground-based measurements at two French sites, *Atmos. Chem. Phys.*, vol. 8, p.
4517-4528, 2008.
- Diffey, B., and McKinlay, A. F.: A reference action spectrum for ultraviolet induced erythema in human skin, *Human
Exposure to UV radiation: Risks and Regulations*, 83-87, Elsevier, NY, 1987.
- 540 GOME-2 Product guide, EUMETSAT, 2011.
- Houët, M.: Spectroradiométrie du rayonnement Solaire UV au sol: Améliorations apportées à l'instrumentation et au
traitement des mesures. Analyse pour l'évaluation du contenu atmosphérique en ozone et en aérosols, Ph.D. thesis, Univ.
of Lille, France, 2003.
- Ialongo, I., Casale, G. R., and Siani, A. M.: Comparison of total ozone and erythemal UV data from OMI with ground-based
545 measurements at Rome station, *Atmos. Chem. Phys.*, 8, 3283– 3289, 2008.
- Kalakoski, N.: O3M SAF Validation Report, Offline UV Index, SAF/O3M/FMI/VR/OUV/091, FMI,
http://o3msaf.fmi.fi/docs/vr/Validation_Report_OUV_Feb_2009.pdf, 2009.
- Kazadzis, S., Bais, A., Arola, A., Krotkov, N., Kouremeti, N., and Meleti, C.: Ozone Monitoring Instrument spectral UV
irradiance products: comparison with ground based measurements at an urban environment, *Atmos. Chem. and Phys.*,
550 vol. 9, p. 585-594, 2009a.
- Kazadzis, S., Bais, A., Balis, D., Kouremeti, N., Zempila, M., Arola, A., Giannakaki, E., Amiridis, V., and Kazantzidis, A.:
Spatial and temporal UV irradiance and aerosol variability within the area of an OMI satellite pixel, *Atmos. Chem. and
Phys.*, vol. 9, p. 4593-4601, 2009b.
- Kinne, S.: Towards an observation-tied AOD climatology, presentation in AT2 Aerosol Workshop, Bremen, June 2007.
- 555 Kinne, S., O'Donnel, D., Stier, P., Kloster, S., Zhang, K., Schmidt, H., Rast, S., Giorgetta, M., Eck, T. F., and Stevens, B. :
MAC-v1: A new global aerosol climatology for climate studies, *J. Adv. Model. Earth Syst.*, 5, 704–740,
doi:10.1002/jame.20035, 2013.
- Köpke, P., M. Hess, I. Schult, and E.P. Shettle: Global Aerosol Data Set, Report No. 243, Max-Planck-Institut für
Meteorologie, Hamburg, ISSN 0937-1060, 1997.



- 560 Krotkov, N.A., Herman, J., Bhartia, P.K., Sefstor, C., Arola, A., Kaurola, J., Taalas, P., and Vasilkov, A.: OMI Surface UV Irradiance Algorithm, in OMI Algorithm Theoretical Basis Document, Volume III: Clouds, Aerosols, and Surface UV Irradiance, ATBD-OMI-03, http://eospsa.gsfc.nasa.gov/eos_homepage/for_scientists/atbd/docs/OMI/ATBD-OMI-03.pdf, 2002.
- Kujanpää, J., Algorithm Theoretical Basis Document, Offline UV (OUV) Products, SAF/O3M/FMI/ATBD/001.FMI, 565 http://o3msaf.fmi.fi/docs/atbd/Algorithm_Theoretical_Basis_Document_OUV_Jun_2013.pdf, 2013.
- Kujanpää, J., and Kalakoski, N.: Operational surface UV radiation product from GOME-2 and AVHRR/3 data, Atmos. Meas. Tech., 8, 4399–4414, doi:10.5194/amt-8-4399-2015, 2015.
- Levelt, P.F., van den Oord, G.H.J., Dobber, M.R., Mälkki, A., Visser, H., de Vries, J., Stammes, P., Lundell, J. O. V., and Saari, H.: The Ozone Monitoring Instrument, IEEE Transactions on Geoscience and Remote Sensing, vol. 44, no. 5, p. 570 1093-1101, 2006.
- McKenzie, R. L., Johnston, P. V., Smale, D., Bodhaine, B. A., and Madronich, S. : Altitude effects on UV spectral irradiance deduced from measurements at Lauder, New Zealand, and at Mauna Loa Observatory, Hawaii, J. Geophys. Res., vol. 106, p. 22845-22860, 2001.
- Munro, R., Lang, R., Klaes, D., Poli, G., Retscher, C., Lindstrot, R., Huckle, R., Lacan, A., Grzegorski, M., Holdak, A., 575 Kokhanovsky, A., Livschitz, J., and Eisinger, M. : The GOME-2 instrument on the Metop series of satellites: instrument design, calibration, and level 1 data processing – an overview, Atmos. Meas. Tech. Discuss., 8, 8645–8700, 2015.
- Muyimbwa, D., Dahlback, A., Ssenyonga, T., Chen, Y.-C., Stammes, J. J., Frette, Ø. , and Hamre, B.: Validation of ozone monitoring instrument ultraviolet index against ground-based UV index in Kampala, Uganda, Appl. Opt., doi.org/10.1364/AO.54.008537, 2015.
- 580 Slaper, H., Reinen, H., Blumthaler, M., Huber, M. and Kuik, F.: Comparing ground-level spectrally resolved solar UV measurements using various instruments: a technique resolving effects of wavelength shift and slit width, Geophys. Res. Lett., 22, 20, 2721-2724, 1995.
- Tanskanen, A.: Lambertian surface albedo climatology at 360 nm from TOMS data using moving time-window technique, Proc. XX Quadrennial Ozone Symposium, June 2004.
- 585 Tanskanen, A., Lindfors, A., Määttä, A., Krotkov, N., Herman, J., Kaurola, J., Koskela, T., Lakkala, K., Fioletov, V., Bernhard, G., McKenzie, R., Kondo, Y., O'Neill, M., Slaper, H., den Outer, P., Bais, A. F., and Tamminen, J.: Validation of daily erythemal doses from Ozone Monitoring Instrument with ground-based UV measurement data, J. Geophys. Res., vol. 112, D24S44, doi: 10.1029/2007JD008830, 2007.
- Weihs, P., Blumthaler, M., Rieder, H.E., Kreuter, A., Simic, S., Laube, W., Schmalwieser, A.W., Wagner, J.E., and 590 Tanskanen, A.: Measurements of UV irradiance within the area of one satellite pixel, Atmos. Chem. and Phys., vol. 8, p. 5615–5626, 2008.
- York, D., Evensen, N. M., López Martínez, M., and De Basabe Delgado, J.: Unified equations for the slope, intercept, and standard errors of the best straight line, American Journal of Physics 72, 367; doi: 10.1119/1.1632486, 2004.



	n	Mean bias UVI	Median bias UVI	RMS UVI	Mean rel bias %	Median rel bias %	rRMS %	Slope (unc.)	Interc. UVI	r
VDA										
OMI-V1.2-SPECTRO	1356	0.57	0.38	0.94	31.5	20.9	54.8	1.17 (0.01)	-0.01	0.95
OMI-V1.3-SPECTRO	1346	0.32	0.21	0.70	22.5	12.5	46.8	1.08 (0.01)	0.00	0.95
GOME-2-SPECTRO	795	0.50	0.33	0.90	20.6	12.1	45.0	1.12 (0.01)	-0.12	0.94
OHP										
OMI-V1.2-SPECTRO	1313	0.91	0.83	1.29	31.3	19.7	57.2	1.14 (0.01)	0.07	0.96
OMI-V1.3-SPECTRO	1283	0.42	0.32	0.89	21.6	9.3	54.6	1.04 (0.01)	0.09	0.96
GOME-2-SPECTRO	1041	0.53	0.41	0.97	19.8	8.4	51.6	1.05 (0.01)	-0.03	0.96
SDR										
OMI-V1.2-SPECTRO	782	1.30	0.80	2.71	27.9	10.7	62.8	0.86 (0.02)	1.61	0.72
OMI-V1.3-SPECTRO	774	1.39	0.78	2.70	29.0	10.4	64.2	0.91 (0.02)	1.36	0.74
GOME-2-SPECTRO	642	1.56	0.87	2.81	34.6	10.8	75.3	0.78 (0.03)	2.45	0.71

595

Table 1. Summary of UVI OMI-GOME-2 validation results at the three sites for distances (Dist) between the station and the CTP/grid cell center point ≤ 100 km and for all-sky conditions. Results for the two OMI versions are presented. n is the number of points, r is the correlation coefficient. We have indicated the slope (uncertainty in parentheses) and intercept (interc.) of the regression line. See the statistics definitions in Appendix.



	n	Mean bias UVI	Median bias UVI	RMS UVI	Mean rel bias %	Median rel bias %	rRMS %	Slope (unc.)	Interc. UVI	r
VDA										
OMI-V1.2-SPECTRO	72	0.71	0.79	0.84	16.8	18.1	17.8	1.20 (0.01)	-0.08	1.00
OMI-V1.3-SPECTRO	72	0.32	0.32	0.40	7.9	8.4	10.2	1.10 (0.01)	-0.06	1.00
GOME-2-SPECTRO	37	0.33	0.39	0.48	5.2	8.3	11.1	1.14 (0.02)	-0.31	0.99
OHP										
OMI-V1.2-SPECTRO	266	0.88	0.90	1.03	16.3	17.2	17.4	1.18 (0.01)	-0.05	1.00
OMI-V1.3-SPECTRO	263	0.26	0.24	0.42	5.5	5.8	8.9	1.05 (0.01)	0.01	0.99
GOME-2-SPECTRO	200	0.24	0.25	0.46	1.8	4.1	9.4	1.09 (0.01)	-0.27	0.99
SDR										
OMI-V1.2-SPECTRO	175	0.29	0.44	1.10	3.6	5.0	11.2	1.02 (0.03)	0.01	0.94
OMI-V1.3-SPECTRO	170	0.30	0.37	0.87	3.5	4.2	9.4	1.03 (0.02)	0.00	0.96
GOME-2-SPECTRO	145	0.18	0.30	0.80	2.5	3.8	8.1	0.98 (0.02)	0.26	0.96

605

Table 2. Same as Table 1 but for CS conditions.



610

	n	Mean bias UVI	Median bias UVI	RMS UVI	Mean rel bias %	Median rel bias %	rRMS %	Slope (unc.)	Interc. UVI	r
VDA										
Dist OMI-V1.3-SPECTRO	349	0.25	0.16	0.61	15.4	10.3	34.8	1.06 (0.02)	-0.01	0.96
Dist GOME-2-SPECTRO	114	0.43	0.28	0.79	15.8	14.3	31.0	1.10 (0.03)	-0.05	0.95
OHP										
Dist OMI-V1.3-SPECTRO	273	0.42	0.34	0.76	19.2	8.3	46.2	1.05 (0.02)	0.06	0.97
Alti OMI-V1.3-SPECTRO	687	0.42	0.32	0.78	21.9	9.3	54.7	1.05 (0.01)	0.07	0.97
Dist GOME-2-SPECTRO	144	0.60	0.49	1.12	22.2	10.3	54.3	0.99 (0.03)	0.09	0.95
SDR										
Dist OMI-V1.3-SPECTRO	341	1.06	0.60	2.41	21.5	8.1	52.7	0.91 (0.03)	1.10	0.75
Alti OMI-V1.3-SPECTRO	576	1.56	0.94	2.83	32.0	11.9	68.3	0.92 (0.03)	1.45	0.74
Dist GOME-2-SPECTRO	93	1.73	1.00	3.17	40.2	11.0	91.5	0.62 (0.09)	3.67	0.60

Table 3. Same as Table 1 but with a filter on the distance between the station and the CTP/grid cell center point (Dist \leq 10 km), and with a filter on OMI CTP_altitude.

At OHP the altitude filter is: Site_altitude - 250 m \leq CTP_altitude \leq Site_altitude + 250 m.

At SDR the altitude filter is: 0 m \leq CTP_altitude \leq Site_altitude + 250 m



	n	Mean bias UVI	Median bias UVI	RMS UVI	Mean rel bias %	Median rel bias %	rRMS %	Slope (unc.)	Interc. UVI	r
VDA										
Dist OMI-V1.3-SPECTRO	14	0.28	0.32	0.36	5.4	6.6	8.0	1.09 (0.01)	-0.08	1.00
Dist GOME-2-SPECTRO	2									
OHP										
Dist OMI-V1.3-SPECTRO	53	0.29	0.25	0.41	5.2	5.3	8.6	1.07 (0.02)	-0.09	0.99
Alti OMI-V1.3-SPECTRO	145	0.29	0.24	0.40	5.8	5.9	8.3	1.05 (0.01)	0.00	1.00
GOME-2-SPECTRO	19	0.23	0.18	0.53	0.3	4.5	11.0	1.11 (0.03)	-0.33	0.99
SDR										
Dist OMI-V1.3-SPECTRO	89	0.13	0.28	0.89	1.8	3.8	9.4	1.00 (0.04)	0.06	0.96
Alti OMI-V1.3-SPECTRO	119	0.41	0.45	0.82	4.7	5.5	9.1	1.05 (0.03)	-0.06	0.98
Dist GOME-2-SPECTRO	16	0.01	0.23	0.89	1.3	3.2	8.0	0.90 (0.07)	0.88	0.96

620

Table 4. Same as Table 3 but for CS conditions



625

	n	Mean bias UVI	Median bias UVI	RMS UVI	Mean rel bias %	Median rel bias %	rRMS %	Slope (unc.)	Interc. UVI	r
VDA										
OMI-V1.3-SPECTRO	681	0.37	0.29	0.72	21.2	12.1	41.8	1.05 (0.01)	0.08	0.95
GOME-2-SPECTRO	681	0.50	0.32	0.89	20.2	12.1	44.6	1.12 (0.02)	-0.12	0.94
OHP										
OMI-V1.3-SPECTRO	821	0.39	0.30	0.83	20.5	8.5	51.9	1.04 (0.01)	0.08	0.96
GOME-2-SPECTRO	821	0.54	0.43	0.97	19.1	8.4	50.6	1.06 (0.01)	-0.06	0.96
SDR										
OMI-V1.3-SPECTRO	523	1.34	0.75	2.66	29.2	10.1	66.7	0.91 (0.03)	1.28	0.74
GOME-2-SPECTRO	523	1.58	0.90	2.84	35.1	11.3	75.5	0.78 (0.03)	2.40	0.70

Table 5. Same as Table 1 but for the same dates for both OMI and GOME-2.

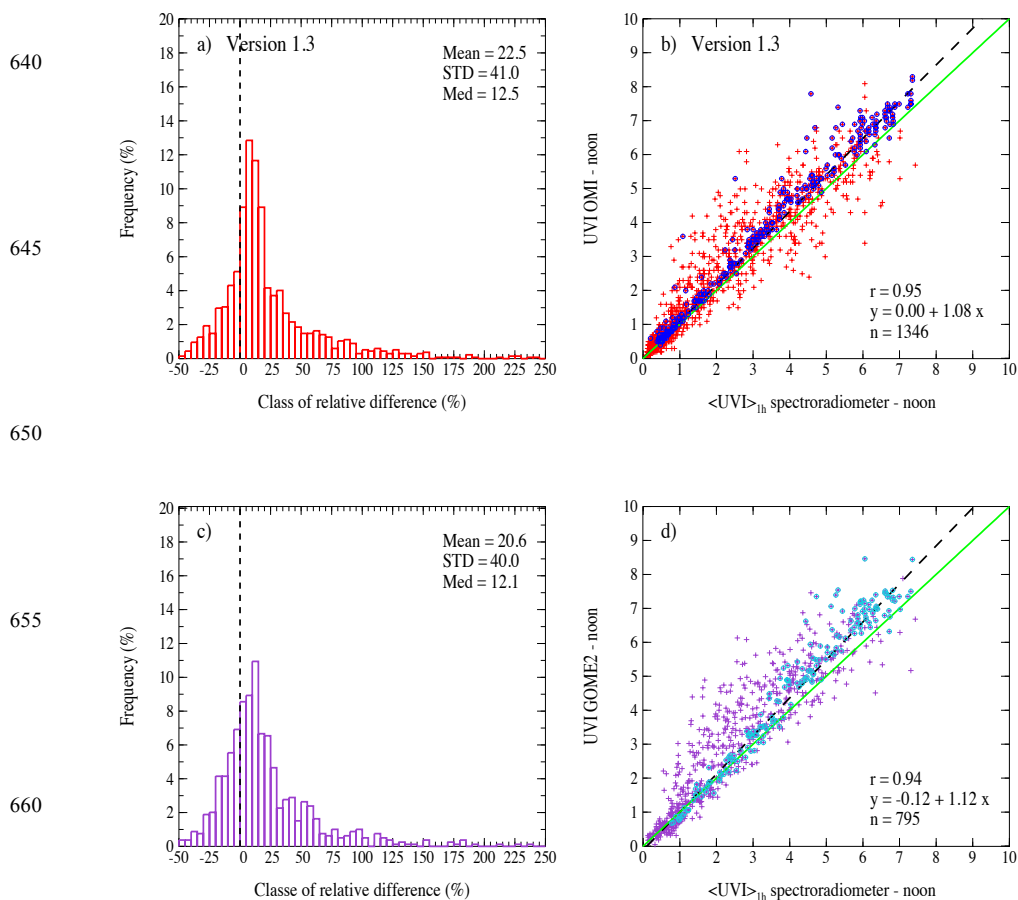
630



	n	Mean bias UVI	Median bias UVI	RMS UVI	Mean rel bias %	Median rel bias %	rRMS %	Slope (unc.)	Interc. UVI	r
VDA										
OMI-V1.3-SPECTRO	37	0.36	0.37	0.41	8.5	8.6	9.8	1.10 (0.01)	-0.07	1.00
GOME-2-SPECTRO	37	0.33	0.39	0.48	5.2	8.3	11.1	1.14 (0.02)	-0.31	0.99
OHP										
OMI-V1.3-SPECTRO	168	0.27	0.23	0.38	5.5	5.4	8.6	1.05 (0.01)	-0.01	0.99
GOME-2-SPECTRO	168	0.26	0.27	0.47	2.2	4.3	9.5	1.09 (0.01)	-0.27	0.99
SDR										
OMI-V1.3-SPECTRO	115	0.29	0.35	0.91	3.6	4.3	9.8	1.02 (0.03)	0.06	0.96
GOME-2-SPECTRO	115	0.14	0.24	0.84	2.2	3.4	8.4	0.97 (0.03)	0.34	0.96

Table 6. Same as Table 2 but for the same dates for both OMI and GOME-2.

635



665 **Figure 1.** OMI-v1.3 (top panels) and GOME-2 (bottom panels) versus GB observations for Dist≤100 km and for AS
666 conditions at VDA. GB measurements are averages over 1 h around local noon. a) and c): histograms of per cent relative
667 difference ($100 \cdot (SB-GB)/GB$) binned with 5 % interval. Few statistics parameters are indicated. b) and d): scatter plots of
668 satellite estimates versus GB measurements. Circled crosses correspond to COD ≤ 1 (COD at overpass for OMI-v1.3, and at
669 noon for GOME-2). The equation of the regression line (dash line) and the correlation coefficient are indicated. The green
670 solid line is the first bisector.

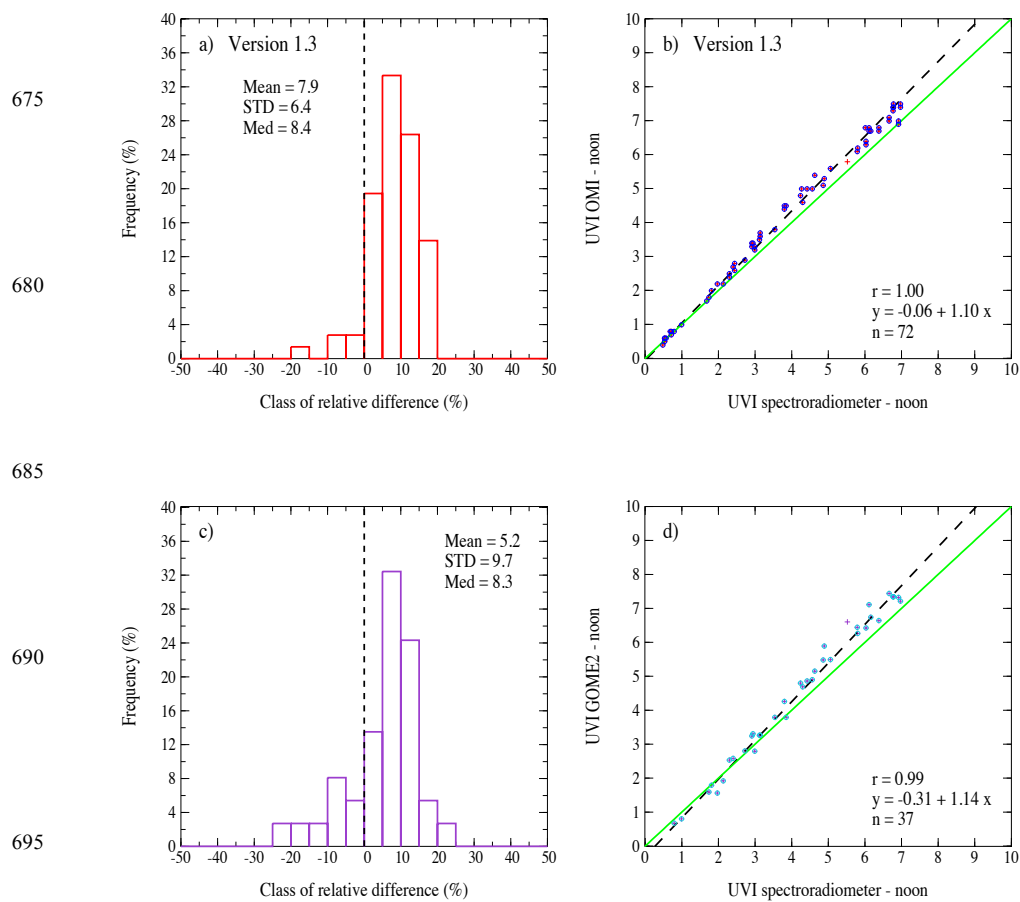


Figure 2. Same as Fig. 1 but for CS conditions at VDA.

700

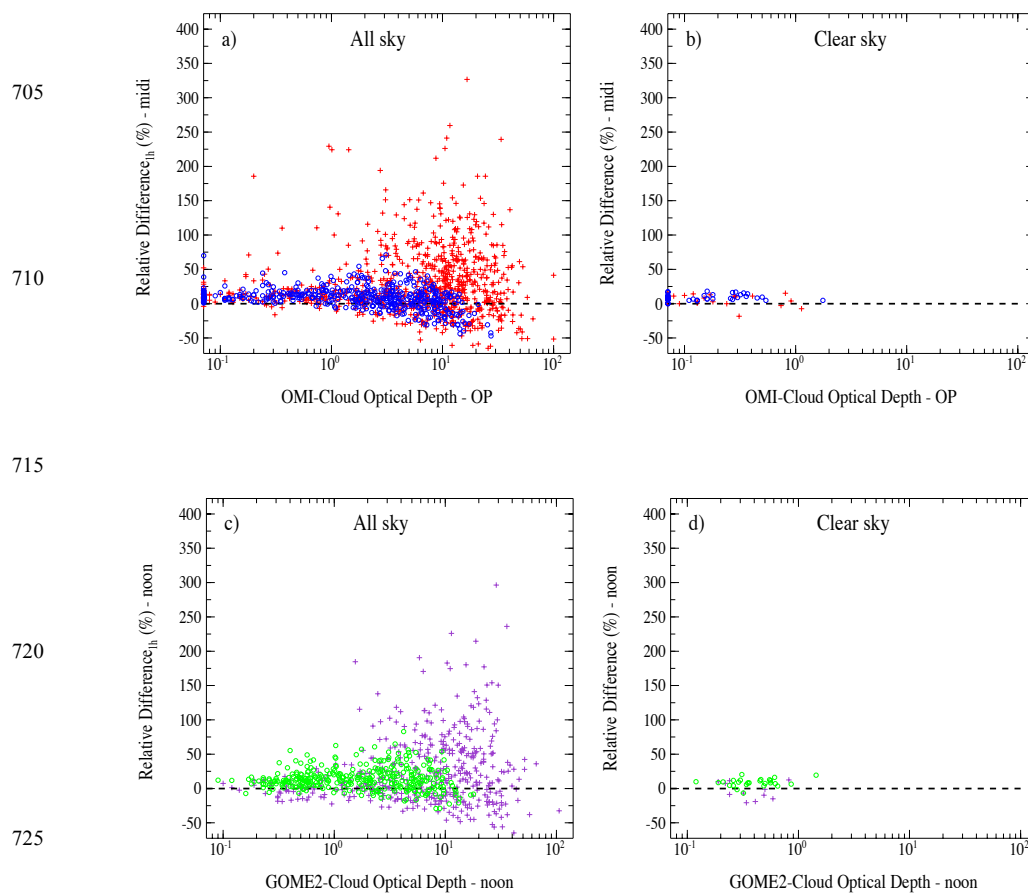


Figure 3. Per cent relative difference versus Cloud Optical Depth (COD) at VDA. COD is given at overpass for OMI-v1.3
730 (top panels), and at noon for GOME-2 (bottom panels). A filtering on the UVI value is made: blue and green circles
720 correspond to UVI(GB value) ≥ 3. Left plots (a and c) for AS conditions, right plots (b and d) for CS conditions.
725



735

740

745

750

755

760

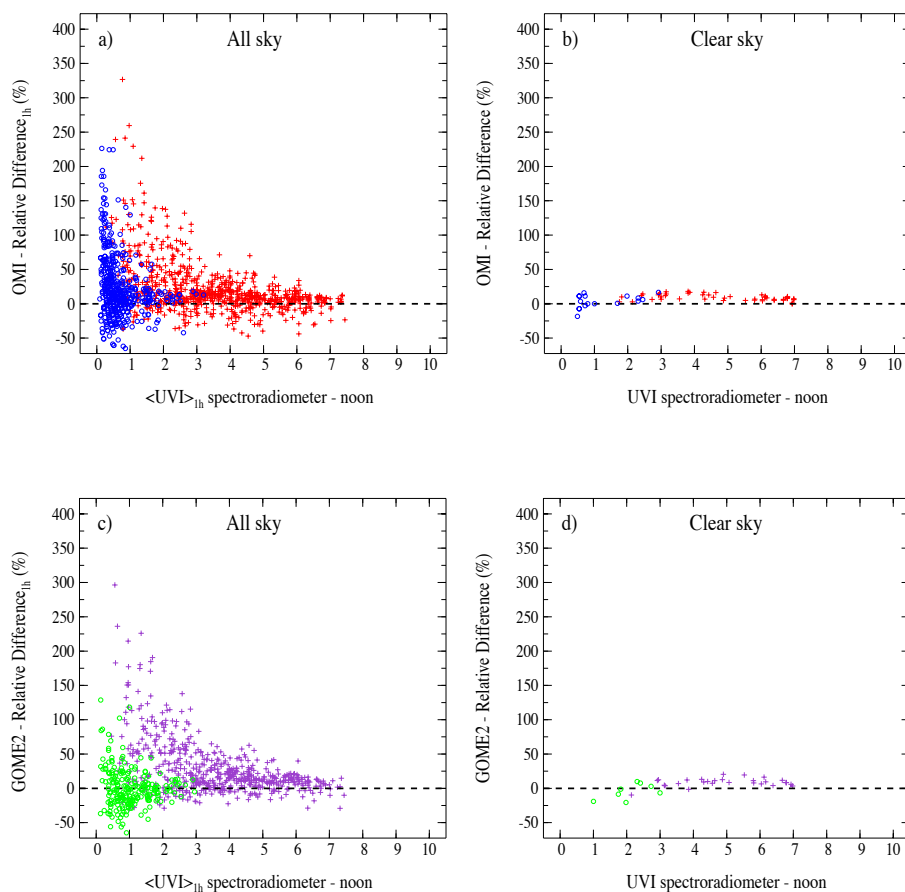


Figure 4. Per cent relative difference versus UVI from GB measurements at VDA for OMI-v1.3 (top panels) and GOME-2 (bottom panels). A filtering on SZA at overpass value is set: blue and green circles correspond to SZA > 60°. Left plots (a and c) for AS conditions, right plots (b and d) for CS conditions.



770

775

780

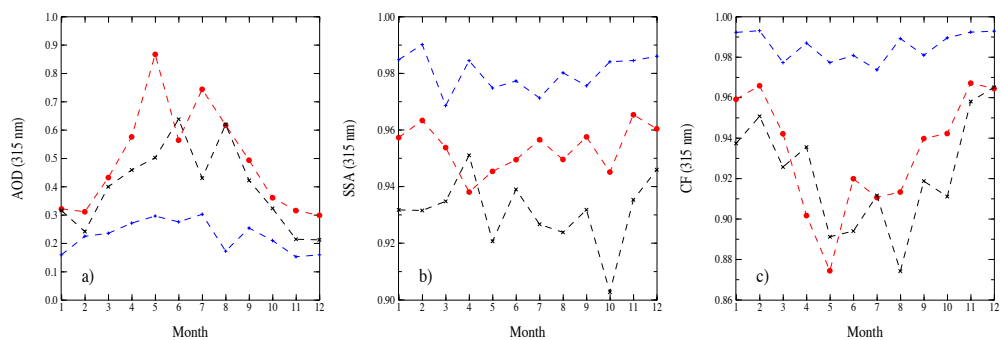


Figure 5. Aerosol data at 315 nm used in the OMI-v1.3 correction for absorbing aerosols. a) AOD ; b) SSA ; c) Correction factor. Red curves are for VDA site, black curves are for OHP and blue curves are for SDR.

785

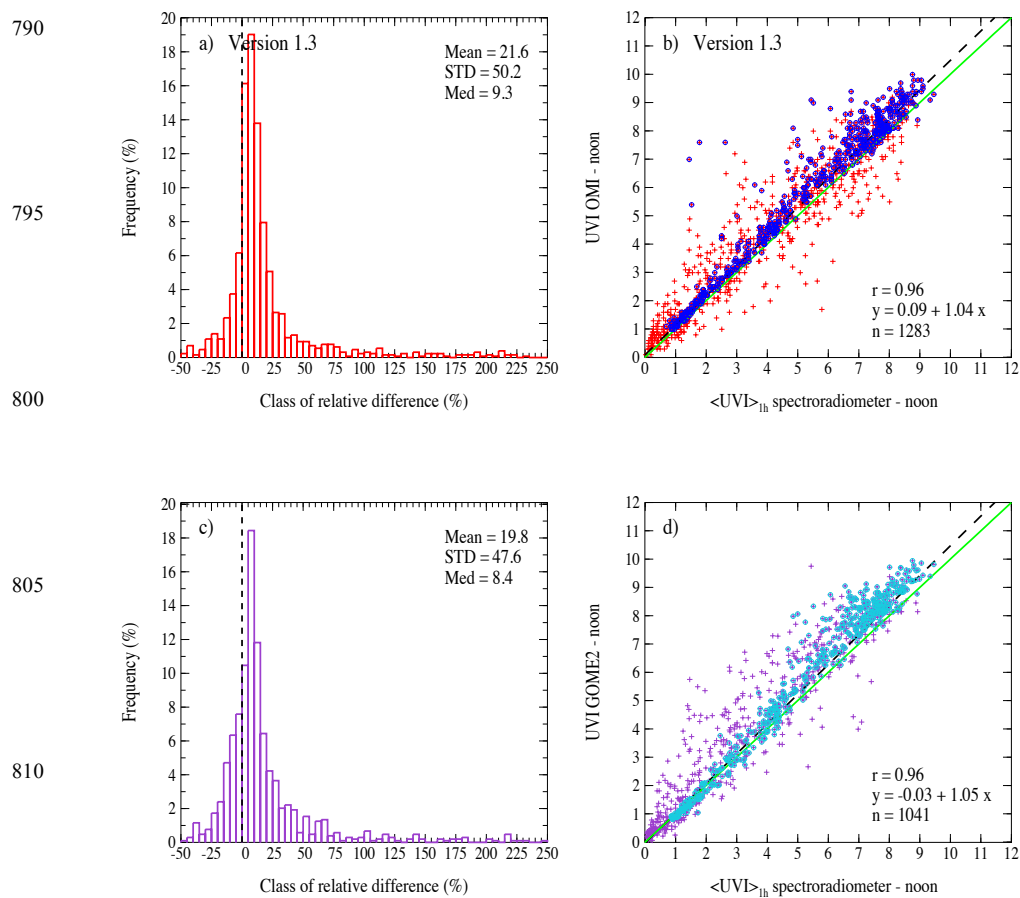
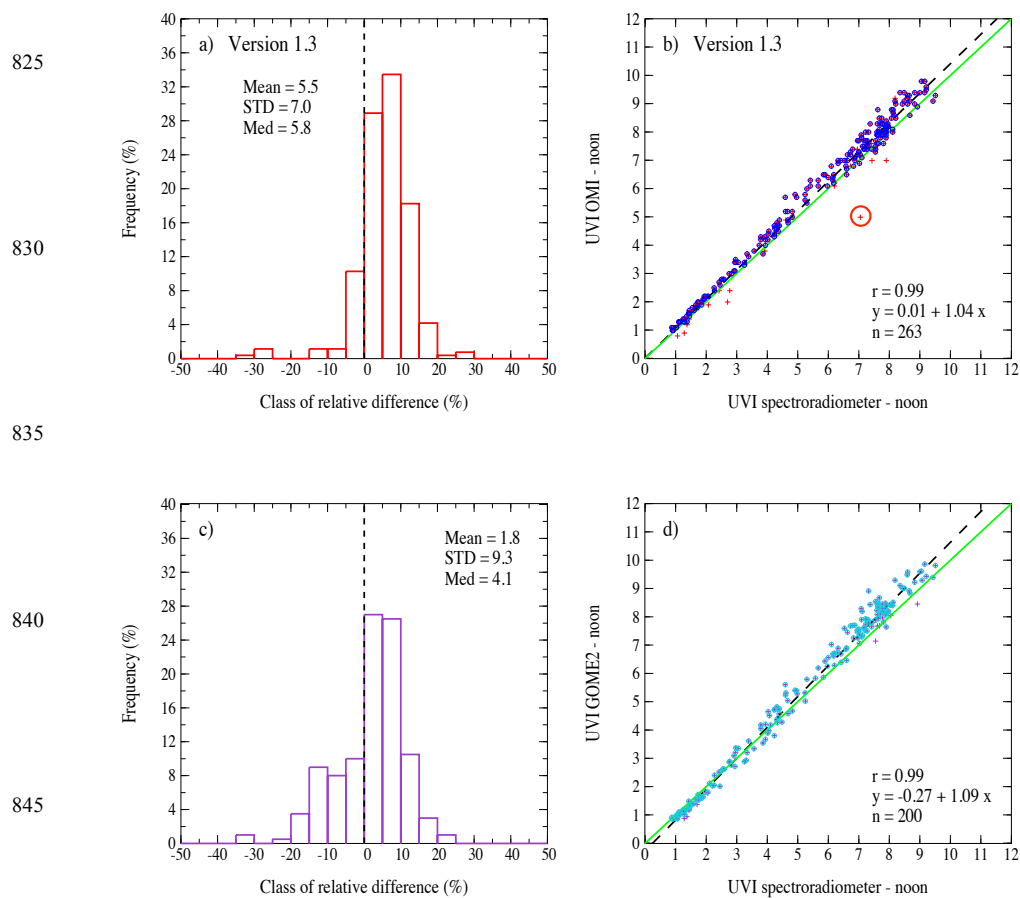


Figure 6. Same as Fig. 1 but for OHP.



850 **Figure 7.** Same as Fig. 2 but for OHP.

855

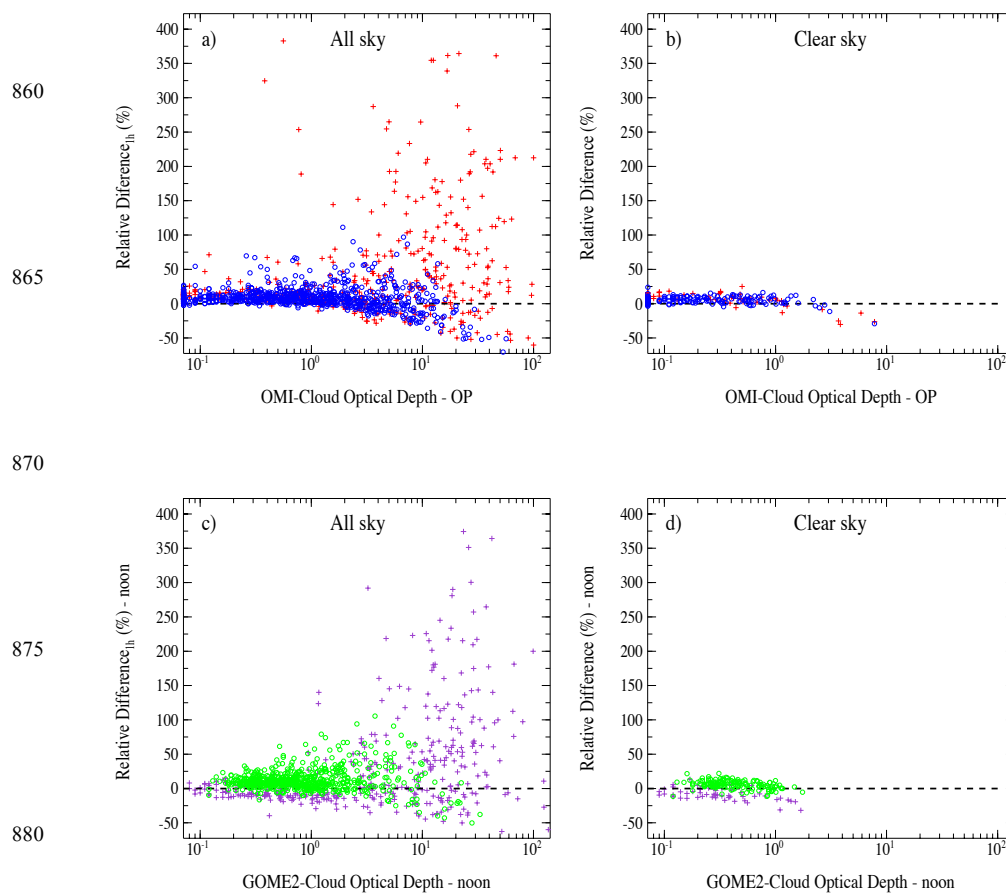


Figure 8. Same as Fig. 3 but for OHP.

885



890

895

900

905

910

915

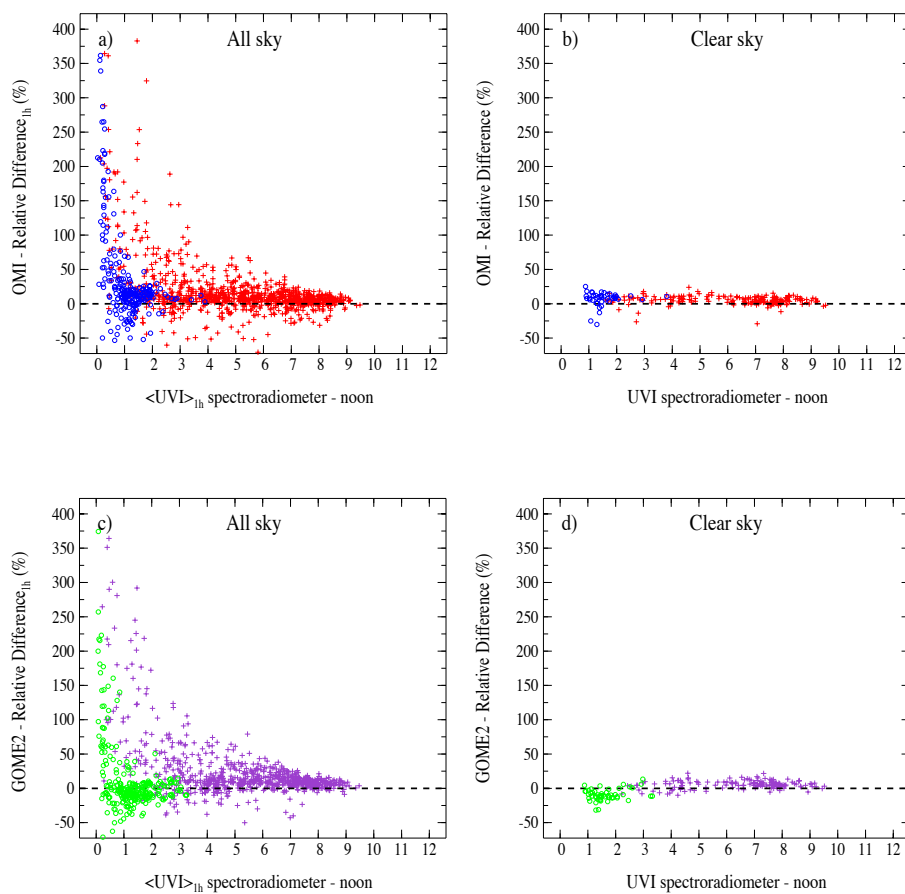


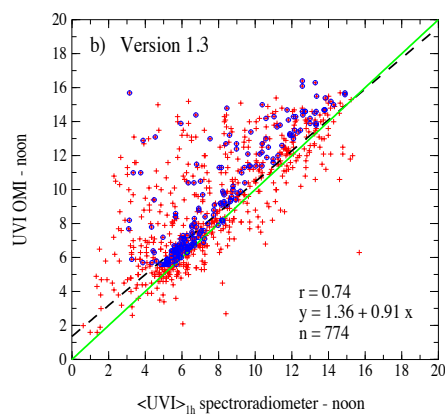
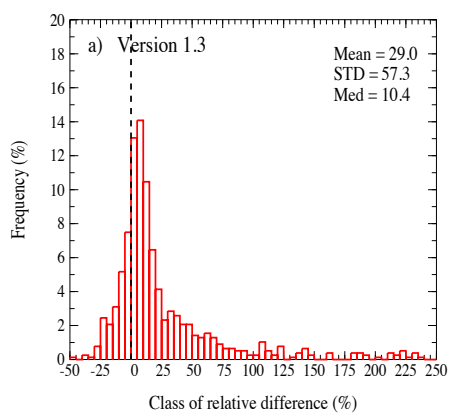
Figure 9. Same as Fig. 4 but for OHP.



920

925

930



935

940

945

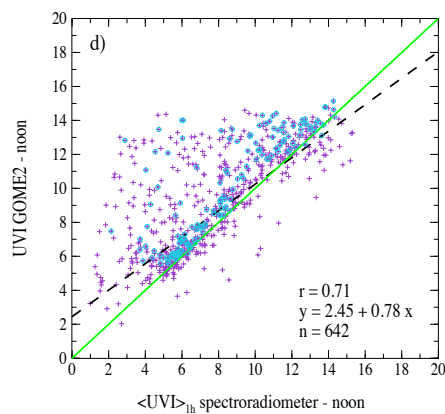
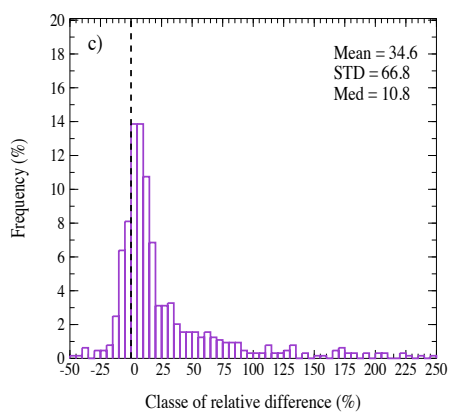


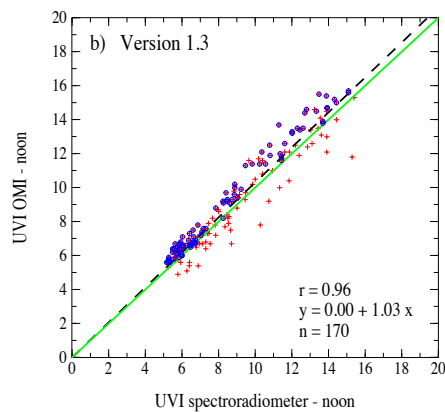
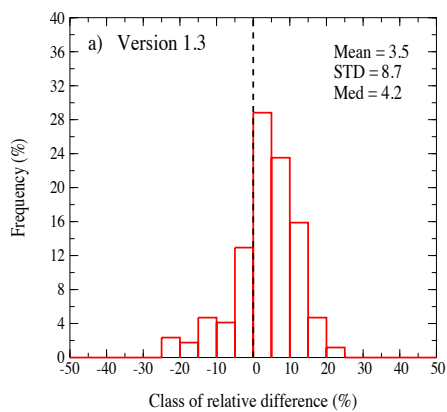
Figure 10. Same as Fig. 1 but for SDR.



950

955

960



965

970

975

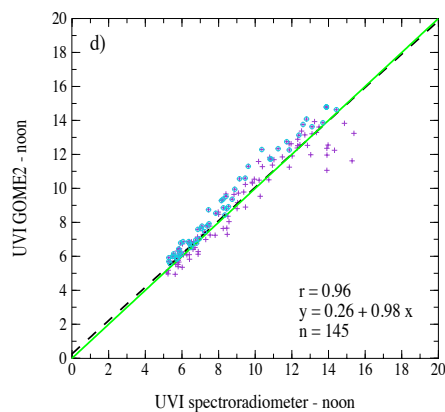
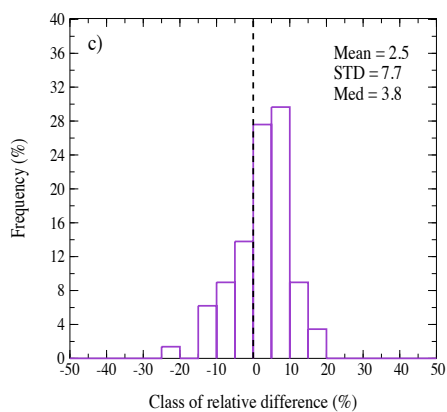


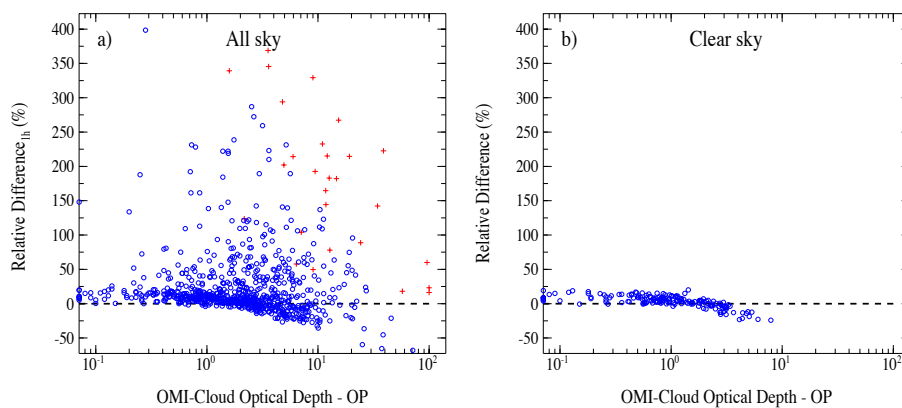
Figure 11. Same as Fig. 2 but for SDR.



980

985

990



995

1000

1005

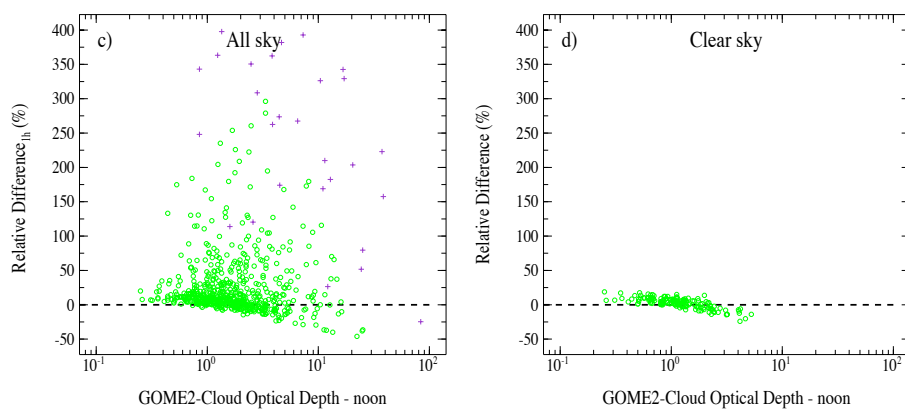


Figure 12. Same as Fig. 3 but for SDR.

1010